J|A|C|S
ARTICLES
Published on Web 02/18/2006

Adsorption and Reaction of CO_2 and SO_2 at a Water Surface

Teresa L. Tarbuck and Geraldine L. Richmond*

Contribution from the Materials Science Institute and Department of Chemistry, University of Oregon, Eugene, Oregon 97403

Received November 5, 2005; E-mail: Richmond@oregon.uoregon.edu

Abstract: The orientation and hydrogen bonding of water molecules in the vapor/water interfacial region in the presence of SO_2 and CO_2 gas are examined using vibrational sum-frequency spectroscopy (VSFS) to gain insight into the adsorption and reactions of these gases in atmospheric aerosols. The results show that an SO_2 surface complex forms when the water surface is exposed to an atmosphere of SO_2 gas. Reaction of SO_2 with interfacial water leads to other spectral changes that are examined by studying the VSF spectra and surface tension isotherms of several salts added to the aqueous phase, specifically $NaHSO_3$, $NaHCO_3$, Na_2SO_3, Na_2CO_3, Na_2SO_4, and $NaHSO_4$. The results are compared with similar studies of CO_2 adsorption and reaction at the surface. A weakly bound surface complex is not observed with CO_2.

Introduction

Understanding the composition, reactivity, and structure of tropospheric aerosols is an essential link to understanding environmental atmospheric chemistry and improving global climate modeling. For example, fundamental studies of the uptake and reactions of SO_2 and CO_2 in water droplets add understanding to atmospheric processes including radiation trapping, radiation scattering, and the formation of cloud condensation nuclei and acid rain.

The uptake of SO_2 and CO_2 in atmospheric aerosols depends on factors including gas-phase diffusion, solubility, mass accommodation probability (the probability of entering the bulk after striking the surface), and reaction rates, which are dependent on additional factors such as pH, droplet size, and temperature. Surface-adsorbed organic materials add yet another level of complexity to these systems.

In the gas phase, SO_2 and CO_2 have different geometries. The addition of SO_2 (CO_2) to water leads to the stepwise reactions:

$$SO_2(aq) \leftrightarrow HSO_3^- + H^+$$
$$HSO_3^- \leftrightarrow SO_3^{2-} + H^+ \quad \text{(I)}$$
$$CO_2(aq) \leftrightarrow HCO_3^- + H^+$$
$$HCO_3^- \leftrightarrow CO_3^{2-} + H^+ \quad \text{(II)}$$

Dissolved in water, SO_2 and CO_2 are in clathrate (gas hydrate) and loosely hydrated structures, respectively.[1] Although SO_2 and CO_2 have similar reactions with water, the reaction products have different geometries and the reaction rates and Henry's law solubilities are also very different (probably because of differences in geometry and size). The first-order rate constants of the reactions for SO_2 and CO_2 with water are 3.4×10^6 and $0.14\ s^{-1}$, respectively,[2] and the Henry's law solubilities are 1.2 and 0.034 mol/L atm, respectively.[3] The Henry's law solubilities for these gases do not take into account any further reactions (acid−base equilibria). The dominant reaction product (SO_2(aq), HSO_3^-, or SO_3^{2-}) depends on the pH of the solution.

Surface complexes have recently been invoked to explain the initial step in a number of surface reaction mechanisms[4−7] including the reaction of SO_2 and water.[8] The SO_2 surface complex is not the dissolved SO_2 species with approximately seven associated water molecules[1] but is SO_2 with fewer associated water molecules because of the proximity to the gas phase. There is an ongoing debate about the existence and composition of SO_2 surface complexes in the interfacial region.[2,8−11] Because the SO_2−water reaction is facile, Jayne et al.[8] assigned the interfacial species as $HSO_3^- - H^+$ to account for the greater SO_2 uptake than that predicted by bulk kinetics at low pH.[8] These results are at odds with later uptake measurements that suggest the uptake coefficients can be determined from the bulk reaction rate constant.[12] Evidence for a surface complex was obtained with second harmonic genera-

* To whom correspondence should be addressed. Phone: 541-346-4635. Fax: 541-346-5859.

(1) Cotton, A. F.; Wilkinson, G. *Advanced Inorganic Chemisty A Comprehensive Text*, 2nd ed.; Interscience: New York, 1966.
(2) Boniface, J.; Shi, Q.; Li, Y. Q.; Cheung, J. L.; Rattigan, O. V.; Davidovits, P.; Worsnop, D. R.; Jayne, J. T.; Kolb, C. E. *J. Phys. Chem. A* **2000**, *104*, 7502−7510.
(3) Finlayson-Pitts, B. J.; Pitts, J. N., Jr. *Chemistry of the Upper and Lower Atmosphere Theory, Experiments, and Applications*; Academic Press: San Diego, 2000.
(4) Knipping, E. M.; Lakin, M. J.; Foster, K. L.; Jungwirth, P.; Tobias, D. J.; Gerber, R. B.; Dabdub, D.; Finlayson-Pitts, B. J. *Science* **2000**, *288*, 301−304.
(5) Hu, J. H.; Shi, Q.; Davidovits, P.; Worsnop, D. R.; Zahniser, M. S.; Kolb, C. E. *J. Phys. Chem.* **1995**, *99*, 8768−8776.
(6) Hanson, D. R.; Ravishankara, A. R. *J. Phys. Chem.* **1994**, *98*, 5728−5735.
(7) George, C.; Behnke, W.; Scheer, V.; Zetzsch, C.; Magi, L.; Ponche, J. L.; Mirabel, P. *Geophys. Res. Lett.* **1995**, *22*, 1505−1508.
(8) Jayne, J. T.; Davidovits, P. *J. Phys. Chem.* **1990**, *94*, 6041−6048.
(9) Yang, H.; Wright, N. J.; Gagnon, A. M.; Gerber, R. B.; Finlayson-Pitts, B. J. *Phys. Chem. Chem. Phys.* **2002**, *4*, 1832−1838.
(10) Donaldson, D. J.; Guest, J. A.; Goh, M. C. *J. Phys. Chem.* **1995**, *99*, 9313−9315.
(11) Bishenden, E.; Donaldson, D. J. *J. Phys. Chem. A* **1998**, *102*, 4638−4642.
(12) Shimono, A.; Koda, S. *J. Phys. Chem.* **1996**, *100*, 10269−10276.

10.1021/ja057375a CCC: $33.50

tion.[10] Subsequent MD simulations[11] suggest that a 1:1, SO_2:H_2O, surface complex is not stable enough to be this species. Recent studies employing ATR-FTIR do not show evidence for the hydrate and estimate less than 4×10^{14} hydrates/cm^2.[9]

Research has been limited to studies of atmospheric molecules in the gas phase because of the lack of suitable surface-specific techniques that can be performed at ambient conditions. However, many of the chemical processes in the lower atmosphere occur in water droplets and are affected by the properties of the interface between the atmosphere and the droplet. For example, one of the first steps in the aqueous oxidation of sulfur dioxide is the transport of SO_2 across the air/water interface.[3] Vibrational sum-frequency spectroscopy (VSFS) and surface tension measurements are powerful tools for investigating interfaces. VSFS probes only those molecules in the interfacial region and can distinguish between SO_2 adsorbate products and surface-active organic contaminates found in aerosols. Surface tension measurements quantify the interfacial species, enabling SF comparisons for equal surface concentrations.

The experiments conducted include VSFS of water surfaces in the presence of SO_2, CO_2, and sodium salts of the reaction and oxidation products. These salts are $NaHSO_3$, $NaHCO_3$, Na_2SO_3, Na_2CO_3, Na_2SO_4, and $NaHSO_4$. Surface tension isotherms of the salt solutions were also acquired. High salt concentrations affect the pH and ionic strength; therefore, spectra of NaOH and HCl at pH 1 and 12, respectively, and spectra of Na_2SO_4 concentrations of constant ionic strength at the vapor/water interface were acquired to examine these effects. The present work builds on our SO_2 study[13] and compares our results with other studies examining the question of an SO_2:H_2O interfacial complex.

Background

VSFS is a suitable technique for studying liquid interfaces because it is surface specific (bulk contributions to the spectrum are forbidden based on symmetry) and because it is selective. It is a vibrational technique giving insights into bond strengths, orientations, and intermolecular interactions of molecules. There is currently significant literature available on the general aspects of the technique.[14−21]

The sum-frequency intensity is proportional to the square of the second-order susceptibility, $\chi^{(2)}$, and the SF spectra must be fit to deconvolve the resonant modes from the nonresonant susceptibility. The inhomogeneous broadening and the homogeneous line widths of the vibrational transitions are accounted for by employing a fitting routine first proposed by Bain:[22]

$$\chi^{(2)} = \chi^{(2)}_{\mathrm{NR}}\, e^{i\varphi} + \sum_{v} \int_{-\infty}^{+\infty} \frac{A_v\, e^{i\phi_v} e^{-[\omega_L - \omega_v/\Gamma_v]^2}}{\omega_L - \omega_{IR} + i\Gamma_L}\, d\omega_L \quad (1)$$

The first term is the nonresonant second-order susceptibility. The second term is a sum over all resonant vibrational modes and is often given the symbol $\chi^{(2)}_{R(v)}$. It represents the convolution of the homogeneous line widths of the individual molecular transitions (HWHM, Γ_L) with inhomogeneous broadening (FWHM, $\sqrt{2\ln 2}\Gamma_v$). The transition strength, A_v, is proportional to the product of the number of molecules and their orientationally averaged IR and Raman transition probabilities. The frequencies of the IR, the Lorentzian, and the resonant modes are ω_{IR}, ω_L, and ω_v, respectively. The phase of each resonant mode is ϕ_v.

Changes in the intensity in the sum-frequency spectrum with concentration can be attributed to a change in the number of molecules, a change in molecular orientation, and/or a change in bond energies. $\chi^{(2)}_{R(v)}$ is dependent on the number of molecules and their orientations in the following way:

$$\chi^{(2)}_{R(v)} = \frac{N}{\epsilon_0}\langle\beta_v\rangle \quad (2)$$

The resonant susceptibility is proportional to N, the number of molecules contributing to the sum-frequency response, and $\langle\beta_v\rangle$, the orientationally averaged molecular susceptibility.

Surface Tension. The interfacial region comprises the area where the number of molecules of solute per unit volume differs from the bulk concentration. Surface tension measurements are a useful tool for acquiring the number density of adsorbates at an interface and allow spectral comparisons between equal surface concentrations. Surface pressure isotherms are fitted to the Gibb's equation[23]

$$\Gamma_i = \frac{1}{nRT}\left(\frac{\partial \pi}{\partial \ln(a_i)}\right)_T \quad (3)$$

to obtain the maximum surface excess. Γ_i is the surface excess concentration at maximum surface coverage (it can be positive or negative) and π is the surface pressure. n is the number of species in excess, and a_i is the activity. For low concentrations, the activity can be replaced with the bulk concentration.

Experimental Section

Laser System. The laser system has been described extensively in previous publications.[24,25] The sum-frequency light is generated by overlapping 800 nm (2 ps, 1 kHz repetition rate) and tunable (2700−4000 cm^{-1}) infrared light in a copropagating geometry at 56° and 67° from the surface normal, respectively. Intensities are approximately 100 μJ of 800 nm light and 4−10 μJ of IR light. After filtering any reflected 800 nm light, the sum-frequency response is collected every 0.0025 μm over the tunable range with a thermoelectrically cooled CCD camera (Princeton Instruments). In these experiments, two polarization combinations are utilized: *ssp* and *sps*. These polarization schemes denote the sum-frequency, visible, and infrared polarizations, respec-

(13) Tarbuck, T. L.; Richmond, G. L. *J. Am. Chem. Soc.* **2005**, *127*, 16806−16807.
(14) Richmond, G. L. *Anal. Chem. News Views* **1997**, *69*, 536A−543A.
(15) Zhu, X. D.; Suhr, H.; Shen, Y. R. *Phys. Rev. B* **1987**, *35*, 3047−3050.
(16) Bloembergen, N.; Pershan, P. S. *Phys. Rev.* **1962**, *128*, 606−622.
(17) Guyot-Sionnest, P.; Hunt, J. H.; Shen, Y. R. *Phys. Rev. Lett.* **1987**, *59*, 1597−1600.
(18) Shen, Y. R. *The Principles of Nonlinear Optics*; Wiley: New York, 1984.
(19) Shen, Y. R. *Mater. Res. Soc. Symp. Proc.* **1986**.
(20) Bain, C. D. *J. Chem. Soc., Faraday Trans.* **1995**, *91*, 1281−1296.
(21) Eisenthal, K. B. *Chem. Rev.* **1996**, *96*, 1343−1360.
(22) Bain, C. D.; Davies, P. B.; Ong, T. H.; Ward, R. N.; Brown, M. A. *Langmuir* **1991**, *7*, 1563−1566.
(23) Chattoraj, D. K.; Birdi, K. S. *Adsorption and the Gibbs Surface Excess*; Plenum Press: New York, 1984.
(24) Gragson, D. E.; McCarty, B. M.; Richmond, G. L.; Alavi, D. S. *J. Opt. Soc. Am. B* **1996**, *13*, 2075−2083.
(25) Allen, H. C.; Raymond, E. A.; Richmond, G. L. *J. Phys. Chem. A* **2001**, *105*, 1649−1655.

tively, which represent polarizations in the plane of incidence (*p*) and normal to the plane of incidence (*s*).

The samples studied are poured or injected via gastight syringes into scrupulously clean glass dishes enclosed in a nitrogen-purged Teflon cell fitted with CaF_2 windows. The Teflon cell has three ports, two of which are used for gases and/or a pressure gauge, and the remaining port is vented via Teflon tubing to a fume hood.

Sample Preparation and Analysis. Gases were purchased from Airgas: SO_2 (lecture bottle, 99.99%), N_2 (cylinder, 99.9%), and CO_2 (cylinder, bone dry, 99.9%). Salt compounds were purchased from Aldrich: Na_2CO_3 (99.995%), Na_2SO_4 (99.99%), $NaHSO_4$ monohydrate (99%), $NaHCO_3$ (minimum 99.5%), Na_2SO_3 (98%), and $NaHSO_3$ (minimum SO_2 content 58.5%) were used as received. In an open container, the $NaHSO_3$ solutions will evolve SO_2 gas because there is an equilibrium between SO_2 (aq), HSO_3^-, and SO_3^{2-}.[10] D_2O (99.9%) was purchased from Cambridge Isotopes. High-purity H_2O was obtained from a Millipore Nanopure system (18 MΩ cm). All salt solutions were injected into the N_2-purged cell via a gastight syringe.

All spectra of the various salt solutions were normalized for variations in SF intensity. The spatial variation between the visible and IR beams when scanning the IR frequency, the temporal lengthening of the IR pulses by water vapor, and the frequency dependence of the optics used for filtering the sum-frequency were removed by dividing the spectra by the nonresonant response from an unprotected gold surface over the same frequency range. To correct for the IR absorbance of the gas, spectra of the vapor (SO_2 and CO_2)/water interfaces were normalized by the nonresonant response from an unprotected gold surface in the presence of the appropriate gas and water vapor. The spectra presented are averages of 2−8 spectra. Often, data were averaged from several samples to improve the signal-to-noise ratio.

The parameters used to fit the neat vapor/water interface in *ssp*-polarization were provided by previous isotopic dilution experiments.[26−28] In these studies, spectra of pure H_2O, increasing concentrations of D_2O in H_2O (HOD), and pure D_2O were iteratively fit as a set allowing all the spectra to be fit with the same peak positions, Lorentzian widths, phases, and similar Gaussian widths. Lorentzian widths are fixed at 5 and 12 for the OH modes and the free OH mode, respectively. The phase relationships are consistent with those reported in molecular dynamics simulations of the neat interface.[27,29] At the neat water interface, the free OH and high-frequency (>3600 cm^{-1}) stretching modes are out of phase with the lower-frequency (<3500 cm^{-1}) modes. Except for the free OH, the Gaussian widths are broad, 100−135 wavenumbers. The parameters used to fit the neat vapor/water interface in *sps*-polarization are the same parameters used for the neat vapor/water *ssp*-polarization spectrum with one exception, an additional resonance at ∼3580 cm^{-1}.

Results and Discussion

The orientation and hydrogen bonding of water molecules at the vapor/water interface in the presence of SO_2 and CO_2 gas are examined to gain insight into gas adsorption and reactions in the interfacial region of atmospheric aerosols. The experiments conducted include VSFS of water surfaces in the presence of SO_2, CO_2, or sodium salts of the reaction and oxidation products. These salts are $NaHSO_3$, $NaHCO_3$, Na_2SO_3, Na_2CO_3, Na_2SO_4, and $NaHSO_4$. Surface tension isotherms of the salts were also acquired. The spectra of the SO_2 (CO_2)/water interface are complex because of the presence of several dissolved reaction products. Therefore, salts of the reaction and oxidation products are employed to examine the effect of each product individually.

To understand the effects of these adsorbates on the water structure, an overview of the water structure is presented first (including spectral assignments). The effect of SO_2 adsorption on the VSFS of the vapor/water interface is examined briefly, followed by studies of related salt solutions containing $NaHSO_3$, Na_2SO_3, $NaHSO_4$, and Na_2SO_4. Then, the SO_2/water interface is discussed in detail in light of the results from the salt studies. Similarly, the results for the CO_2/water interface and the salts of the reaction between CO_2 and water ($NaHCO_3$, Na_2CO_3) are presented. This is followed by a summary of the interpretation of the SO_2 (CO_2)/water interface with contributions from the reaction products and implications for understanding atmospheric aerosols.

Interfacial Water Assignments, Structure, and Orientation. Recent discoveries have led to a molecular picture of the vapor/water interface,[27−36] including a small interfacial depth, ∼6−9 Å,[27,35] and an average coordination of water molecules decreasing from ∼3.6 bonds per molecule in the bulk to ∼2 bonds per molecule at the topmost surface layer.[35] The intermolecular oxygen−oxygen distance expands as one moves from the bulk to the surface.[37] This region of anisotropy includes less water coordination, less hydrogen bonding in the topmost surface layer, and tetrahedrally coordinated water molecules deeper in the interfacial layer.

A spectrum of the neat vapor/water interface in *ssp*- and *sps*-polarization is shown in Figure 1 along with the fitted resonant modes. The assignments of the interfacial OH stretching modes were determined from interfacial isotopic dilution experiments[26−28] which take into account the degree of hydrogen bonding and the surrounding environment. The results are employed here, and the current data are fit with similar parameters obtained from these previous studies. The nonresonant component (not shown) has been taken into account in the analysis. The topmost surface water molecules with the weakest neighboring bonding interactions occur in the 3500−3700 cm^{-1} region of the spectrum. As the amount of cooperative OH stretching between adjacent water molecules increases, the vibrational frequency decreases. Water molecules exhibiting intensity at ∼3400 cm^{-1} and lower energies correspond to water molecules a few angstroms into the liquid, which bond with additional coordination and cooperative interactions.

In the topmost interfacial layer, the sharp feature found at 3700 cm^{-1} corresponds to the free OH that points into the air with its adjacent companion OH mode (which we refer to as the donor mode) pointing into the liquid phase. Calculations by Buch[30] and from our group[38] indicate that intensity for the mode near 3460 cm^{-1} weakly interacts with neighboring water

(26) Raymond, E. A.; Richmond, G. L. *J. Phys. Chem. B* **2004**, *108*, 5051−5059.
(27) Raymond, E. A.; Tarbuck, T. L.; Brown, M. G.; Richmond, G. L. *J. Phys. Chem. B* **2003**, *107*, 546−556.
(28) Raymond, E. A.; Tarbuck, T. L.; Richmond, G. L. *J. Phys. Chem. B* **2002**, *106*, 2817−2820.
(29) Morita, A.; Hynes, J. T. *Chem. Phys.* **2000**, *258*, 371−390.
(30) Buch, V. *J. Phys. Chem. B* **2005**, *109*, 17771−17774.
(31) Du, Q.; Superfine, R.; Freysz, E.; Shen, Y. R. *Phys. Rev. Lett.* **1993**, *70*, 2313−2316.
(32) Wilson, K. R.; Cavalleri, M.; Rude, B. S.; Schaller, R. D.; Nilsson, A.; Pettersson, L. G. M.; Goldman, N.; Catalano, T.; Bozek, J. D.; Saykally, R. J. *J. Phys.: Condens. Matter* **2002**, *14*, L221-L226.
(33) Morita, A.; Hynes, J. T. *J. Phys. Chem. B* **2002**, *106*, 673−685.
(34) Vassilev, P.; Hartnig, C.; Koper, M. T. M.; Frechard, F.; van Santen, R. A. *J. Chem. Phys.* **2001**, *115*, 9815−9820.
(35) Dang, L. X.; Chang, T.-M. *J. Chem. Phys.* **1997**, *106*, 8149−8159.
(36) Goh, M. C.; Hicks, J. M.; Kemnitz, K.; Pinto, G. R.; Bhattacharyya, K.; Eisenthal, K. B.; Heinz, T. F. *J. Phys. Chem.* **1988**, *92*, 5074−5075.
(37) Wilson, K. R.; Schaller, D. T. C.; Saykally, R. J.; Rude, B. S.; Catalano, T.; Bozek, J. D. *J. Chem. Phys.* **2002**, *117*, 7738−7744.
(38) Walker, D.; Richmond, G. L. Manuscript in preparation, 2006.

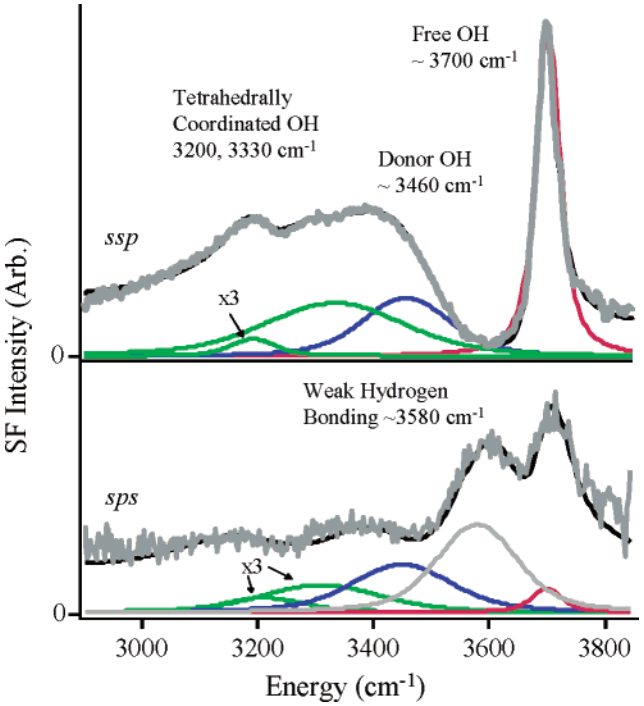

Figure 1. Sum-frequency spectra of the neat vapor/water interface acquired under *ssp*- and *sps*-polarizations. Fitted peaks are shown below the spectra. The nonresonance response is not shown, although it is included in the fit.

molecules as a proton and single electron pair donor. The frequency of this companion donor OH mode is similar to that found for the OH of uncoupled HOD in liquid water.[39,40] Both the free OH and donor OH modes appear in the *ssp*- and *sps*-polarization spectra and represent more than 20% of the surface water molecules.[31] The third dominant species in this weakly bonded topmost surface region is apparent in the *sps*-polarization spectrum near 3580 cm^{-1}. On the basis of MD simulations by Buch[30] and in agreement with our calculations,[38] we attribute this peak to water molecules residing nearly parallel to the interface in the topmost layer that form one to three hydrogen bonds with other species. Pertinent to the discussion below, water molecules solvating surface ions are also found in this high-energy region.

Intensity below this region corresponds to interfacial water molecules a few angstroms from the top layer that have a larger number of bonds per molecule and can interact cooperatively with the extended water network.[27,30] The OH stretching of these collective tetrahedrally coordinated water molecules and the more highly coordinated donor mode occur at 3330 and 3200 cm^{-1}. Note that after the removal of the nonresonant response the signal from these stronger hydrogen-bonded water molecules is relatively small. However, the orientation and bonding of these more strongly bonded interfacial water molecules are very sensitive to surface dipole and electric field effects that extend the surface region to allow more tetrahedrally coordinated water molecules to contribute to the VSFS response. These field effects have been studied extensively,[41,42] and the assignments are supported by IR and Raman data from bulk water that assign the strong intensity in the 3200−3450 cm^{-1} range to stretching

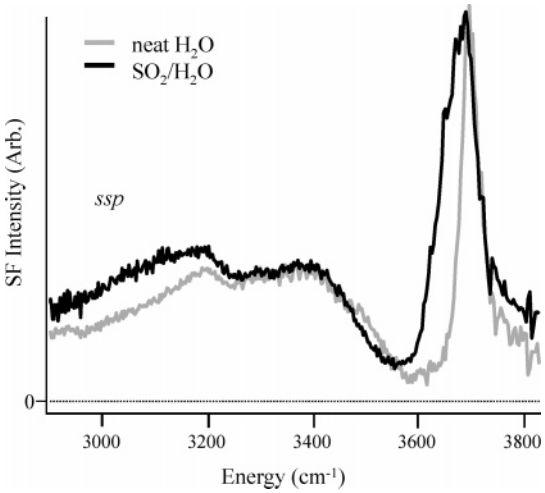

Figure 2. Sum-frequency spectrum of SO_2 gas at the vapor/water interface in the OH stretch region in *ssp*-polarization (black). A neat vapor/water spectrum (gray) is shown for comparison.

of tetrahedrally coordinated water molecules in various hydrogen-bonding environments.[40,43−45] Although not present at the neat vapor/water interface, strong hydrogen bonding and cooperative motion of hydrogen bonds give rise to a spectral feature at ~3150 cm^{-1}. This feature has been observed in spectra of the vapor/ice interface[46] and the interface of strong acid solutions.[47]

Preview of SO_2 Effects on Water Structure at the Interface. An *ssp*-polarization spectrum of the neat vapor/water interface (gray) and the vapor/water interface in the presence of SO_2 gas (black) is shown in Figure 2. Clearly, the neat vapor/water interface is affected by the presence of SO_2 gas. Within seconds of exposure to SO_2, a broadening and red shift of the free OH resonance (to ~3675 cm^{-1}) and an increase in the SF intensity in the tetrahedrally coordinated OH stretching region at 3200 and 3330 cm^{-1} are detected. Deducing the source of these changes in the spectrum is complicated because of the reaction of SO_2 with water at the interface. When SO_2 dissolves in water, a portion is converted to HSO_3^-, and to SO_3^{2-} in milliseconds,[3] decreasing the bulk pH. From the bulk pH of ~1 measured in our experiments and from published values of the equilibrium constants,[3] the SO_2(aq), HSO_3^-, and SO_3^{2-} concentrations are ~0.8, 0.1, and 8×10^{-5} M, respectively. To better understand the changes due to SO_2 at the vapor/water interface, we investigated the change in the surface spectrum in the presence of sodium salts of the reaction products (HSO_3^- and SO_3^{2-}) and the oxidation products (HSO_4^- and SO_4^{2-}). We revisit the SO_2 vapor/water interface after a discussion of the separate influences of the salts, pH, and ionic strength on the vapor/water interface.

$NaHSO_3$, Na_2SO_3, $NaHSO_4$, and Na_2SO_4 Influences on the Structure and Hydrogen Bonding of Water at the Vapor/Water Interface. A concentration series of salts of the reaction and oxidation products of SO_2, $NaHSO_3$, Na_2SO_3, $NaHSO_4$, and

(39) Wall, T. T.; Horning, D. F. *J. Chem. Phys.* **1965**, *43*, 2079−2087.
(40) Scherer, J. R.; Go, M. K.; Kint, S. *J. Phys. Chem.* **1974**, *78*, 1304−1313.
(41) Gragson, D. E.; Richmond, G. L. *J. Phys. Chem. B* **1998**, *102*, 3847−3861.
(42) Richmond, G. L. *Chem. Rev.* **2002**, *102*, 2693−2724.
(43) Scherer, J. R. In *Advances in Infrared and Raman Spectroscopy*; Clark, R. J. H., Hester, R. E., Eds.; Heyden: Philadelphia, 1978; Vol. 5, pp 149−216.
(44) Walrafen, G. E.; Hokmabadi, M. S.; Yang, W.-H. *J. Chem. Phys.* **1986**, *85*, 6964−6969.
(45) Walrafen, G. E.; Fisher, M. R.; Hokmabadi, M. S.; Yang, W.-H. *J. Chem. Phys.* **1986**, *85*, 6970−6982.
(46) Wei, X.; Miranda, P. B.; Shen, Y. R. *Phys. Rev. Lett.* **2001**, *86*, 1554−1557.
(47) Schnitzer, C.; Baldelli, S.; Shultz, J. J. *J. Phys. Chem. B* **2000**, *104*, 585−590.

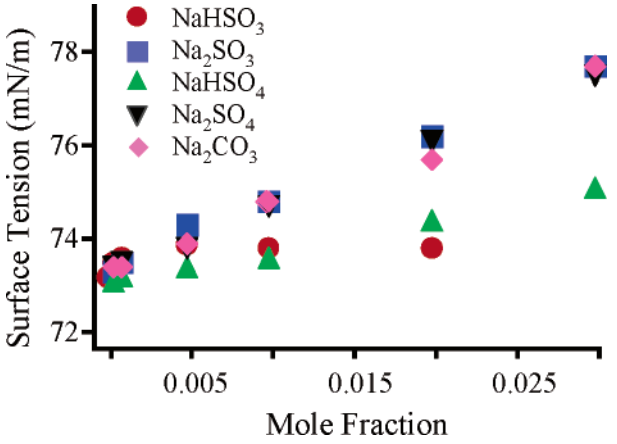

Figure 3. Surface tension for increasing mole fractions of $NaHSO_3$, Na_2SO_3, $NaHSO_4$, Na_2SO_4, and Na_2CO_3.

Na_2SO_4, have been examined using VSFS and surface tension isotherms. They were investigated as sodium salts because sodium ions are small, relatively unpolarizable, and have much less of an effect on the bulk water structure than the anions.[48,49] Sodium ions are expected to have less of an effect on the neat vapor/water interface than protons because they are not as strongly hydrated and they associate more with the anions for a smaller separation of charge.[47] The dominant changes to the resonant modes at the vapor/water interface in the presence of the above four anions in solution are presented below with the spectra of Na_2SO_3, Na_2SO_4, and $NaHSO_4$, demonstrating the changes to the polarizability of the interface, the ionic strength, and the pH, respectively.

These salts are simple electrolytes that increase the surface tension of water (the interfacial ion concentration is less than the bulk concentration), and in the Hofmeister series, which ranks ions on the basis of their effect on the surrounding water structure, they are classified as structure makers. This ion behavior is attributed to the presence of the large polarizable anions that are capable of strong ion−dipole interactions, which influence the structuring and bonding of interfacial water molecules. Surface properties differ from bulk properties even when similar charges are present because of the different geometry and charge distribution at the interface. In Figure 3, Na_2SO_3 and Na_2SO_4 have the largest increase in surface tension, with $NaHSO_3$ and $NaHSO_4$ having similar small increases in surface tension with increasing concentration. (Surface concentrations at 0.02 *X* are all approximately the same order of magnitude (7×10^{13} molecules/cm^2) which is important because it allows direct comparison of all the salt spectra.) Our surface tension measurements of $NaHSO_3$ are only reported up to 0.02 *X* because the SF spectra of solutions above this concentration always show CH stretching modes from an accumulation of adsorbed organics. Although $NaHSO_3$ salt solutions were difficult to keep clean, the trend in surface tension results is in qualitative agreement with Hoppe et al.[50] and is consistent with other inorganic electrolyte solutions. We note that Donaldson reports a decrease in surface tension which stablilizes after approximately 20 min, and this surface tension drop is substantial, to ∼35 mN/m for 3 molal solutions.[10] When contaminants are present in our experiments, the same drop in surface tension occurs.

$NaHSO_3$ and Na_2SO_3. Spectra of $NaHSO_3$ and Na_2SO_3 at the vapor/water interface in *ssp*-polarization are presented in Figure 4 which includes the neat vapor/water interface, 0.005, 0.01, and 0.02 *X* $NaHSO_3$ (4a); the neat vapor/water interface, 0.001, 0.005, 0.01, 0.02, and 0.03 *X* Na_2SO_3 (4b); and the fitted resonant modes for the highest salt concentrations (4c and 4d). The fits presented in Figure 4c,d are from a global fit to the entire concentration series; although not as rigorous as the isotopic dilution global fit that the starting parameters are taken from, it can be used to qualitatively determine trends. Both salts react to a small extent with water, resulting in a pH of approximately 3.5 and 11 for $NaHSO_3$ and Na_2SO_3 at 0.02 and 0.03 *X*, respectively. (These changes in pH will be discussed in more detail when the $NaHSO_4$ data are presented.) Because $NaHSO_3$ samples were under a continuous flow of N_2 during these experiments, the solution was not in equilibrium and evolved SO_2 gas based on the equilibrium among SO_2(aq), HSO_3^-, and SO_3^{2-};[10] however, the SO_2 released during the time of the experiment was not detected in the spectra. Two spectral regions are discussed below: water molecules in highly coordinated tetrahedral or near tetrahedral bonding environments that contribute to symmetric OH stretching (3100−3400 cm^{-1}) and water molecules in the top surface layer either straddling the interface or with fewer bonded sites typical of molecules in asymmetric bonding environments (3500−3700 cm^{-1}). This is followed by a discussion of changes in the nonresonant response.

The increase in spectral intensity for these two salts is primarily from ∼3100−3400 cm^{-1}, indicating that ions are present in the interfacial region. An increase in both the 3200 and 3330 cm^{-1} peaks is observed with the appearance of an additional peak at 3150 cm^{-1} which is most prominent at higher concentrations. There are several possible contributions to this increase: strong ion−dipole interactions that can increase the transition strength of the vibrations of interfacial water molecules, greater water dipole alignment along the surface normal, and increased interfacial depth that the VSF probes due to an increased electric field. Strong ion−dipole interactions are expected to contribute to the increase in spectral intensity because the negative ions are all relatively large, polarizable, and capable of hydrogen bonding to water molecules. As expected, the greater charge on the SO_3^{2-} anion has a greater effect on the water structure than the HSO_3^- anion.

Interestingly, these intensity changes are significantly larger than those found in VSF studies of solutions containing similar concentrations of sodium halide salts.[26,51,52] The greater changes are mostly likely due to the anion's greater size and differing geometry. A small electric field due to the separation of cations and anions is likely present at the interface, which would lead to increased water dipole orientation, increased interfacial depth, and subsequent VSF response for *ssp*-polarization. The phases of the fitted spectral resonances do not change with addition of these salts, indicating that the surface water molecules do not significantly change their orientation with salts present. SF

(48) *Water a Comprehensive Treatise*; Franks, F., Ed.; Plenum Press: New York, 1973; Vol. 3, pp 1−472.
(49) Cacace, M. G.; Landau, E. M.; Ramsden, J. J. *Q. Rev. Biophys.* **1997**, *30*, 241−277.
(50) Hoppe, H.; Enge, G.; Winkler, F. *Z. Chem*. **1976**, *16*, 165−165.
(51) Mucha, M.; Frigato, T.; Levering, L. M.; Allen, H. C.; Tobias, D. J.; Dang, L. X.; Jungwirth, P. *J. Phys. Chem. B* **2005**, *109*, 7617−7623.
(52) Liu, D.; Gang, M.; Levering, L. M.; Allen, H. C. *J. Phys. Chem.* **2004**, *108*, 2252−2260.

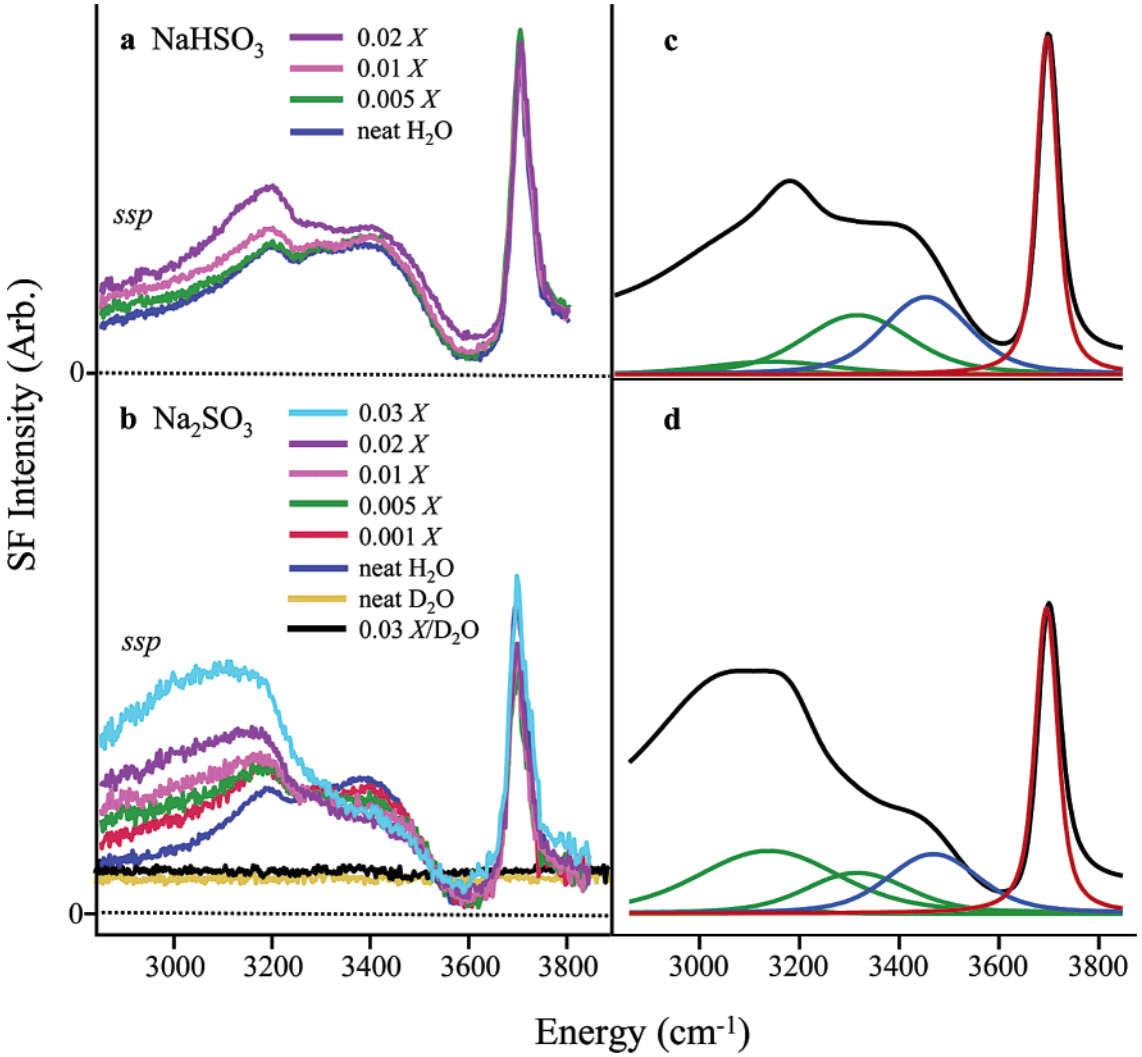

Figure 4. (a) Sum-frequency spectra of $NaHSO_3$ at 0.0, 0.005, 0.01, and 0.02 bulk *X* in the OH stretching region at the vapor/H_2O interface acquired under *ssp*-polarizations. (b) Sum-frequency spectra of Na_2SO_3 at 0.0, 0.005, 0.01, 0.02, and 0.03 bulk *X* and spectra of the neat D_2O and 0.03 *X* Na_2SO_3/D_2O interfaces in the OH stretching region at the vapor/H_2O interface acquired under *ssp*-polarization. (c) Resonant modes and overall fit to 0.02 bulk *X* $NaHSO_3$. (d) Resonant modes and overall fit to 0.03 bulk *X* Na_2SO_3.

studies of acids in solution, H_2SO_4[53] and HNO_3,[54] attributed the change in intensity in this region to the electric double layer. In these studies, increasing the concentration initially increased the intensity in the coordinated OH stretching region; however, the trend reversed near 0.05 *X*, and the intensity in the coordinated OH stretching region decreased. The trend reversal was attributed to tightening of the electric double layer.

Changes in the intensity in the weakly bonded region (3500−3700 cm^{-1}) are measurable but small in comparison to the stronger highly coordinated OH stretching region. Qualitatively examining the spectrum of 0.02 *X* $NaHSO_3$, the dip at ∼3600 cm^{-1} appears to be filling in. This spectral change can be fit with a broadened peak at 3460 cm^{-1}, in the region of the donor OH mode (see fitted modes in 4c), or fit with an additional resonance possibly from the effect of protons in the interfacial region.[55] This indicates that water molecules in the top surface layer where fewer hydrogen bonds are present are influenced by the dissolution of $NaHSO_3$, even though there is no significant measurable change in the fitted free OH intensity.

The presence of SO_3^{2-} ions in solution has no significant effect on the free OH intensity at low concentrations. At ≥0.02 *X* Na_2SO_3, the free and donor OH modes slightly decrease in intensity, which we attribute to water molecules in the uppermost layer that reorient to solvate the anions and/or are displaced by the large solvated anions. This is supported by fits to the data at high concentrations of Na_2SO_3 that improve slightly with a very small resonance at 3645 ± 50 cm^{-1}. This high-frequency mode is attributed to weak interactions typical of water molecules solvating interfacial ions. These high-frequency features have been seen at several interfaces and in bulk solutions with ions present.[26,56−59] A similar solvation feature occurs at ∼3650 cm^{-1} in isotopic dilution studies with sodium halide solutions.[26] Bulk IR and Raman studies of sodium halide

(53) Baldelli, S.; Schnitzer, C.; Shultz, M. J.; Campbell, D. J. *J. Phys. Chem. B* **1997**, *101*, 10435−10441.
(54) Schnitzer, C.; Baldelli, S.; Campbell, D. J.; Schultz, M. J. *J. Phys. Chem. A* **1999**, *103*, 6383−6386.
(55) Petersen, M. K.; Iyengar, S. S.; Day, T. J. F.; Voth, G. A. *J. Phys. Chem. B* **2004**, *108*, 14804−14806.
(56) Scatena, L. F.; Richmond, G. L. *Chem. Phys. Lett.* **2004**, *383*, 491−495.
(57) Strauss, I. M.; Symons, M. C. R. *J. Chem. Soc., Faraday Trans.* **1978**, *1*, 2518−2529.
(58) Walrafen, G. E. *J. Chem. Phys.* **1971**, *55*, 768−792.
(59) Tarbuck, T. L.; Richmond, G. L. *J. Phys. Chem. B* **2005**, *109*, 20868−20877.

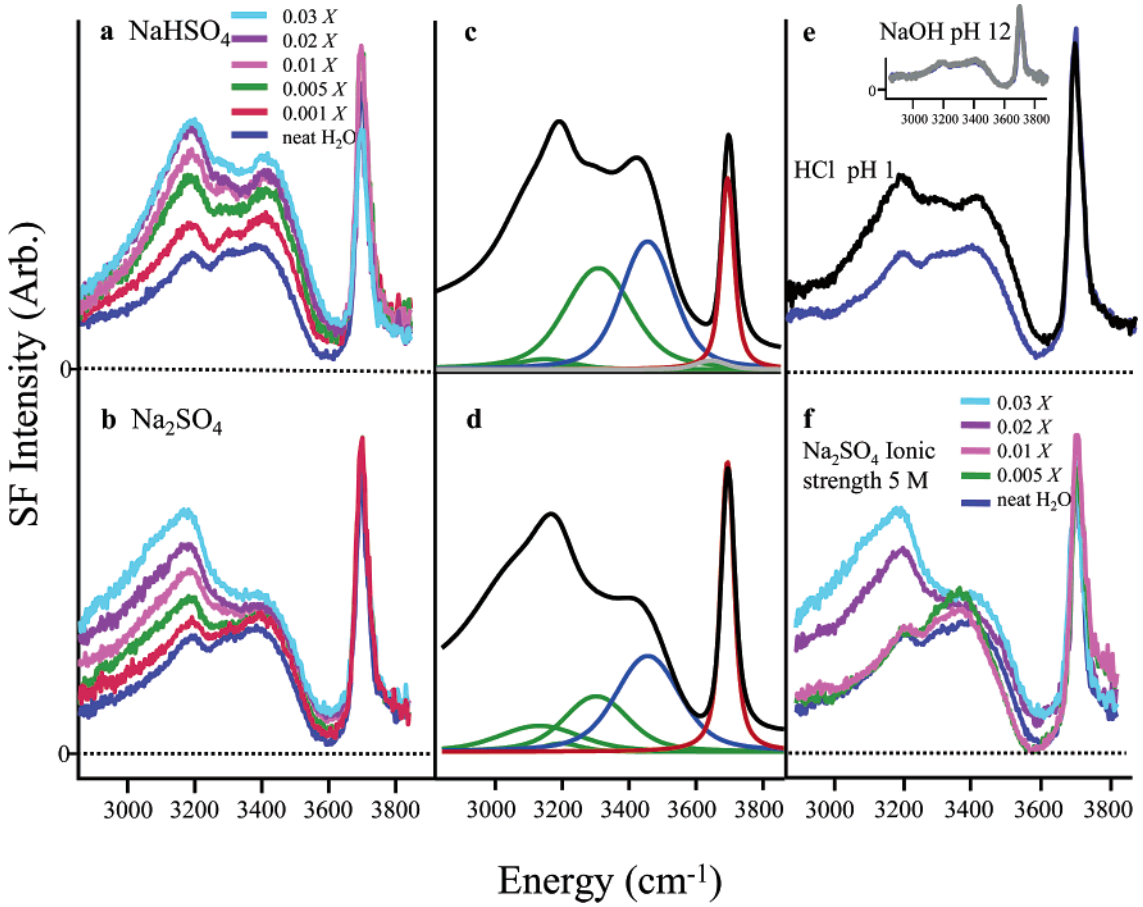

Figure 5. Sum-frequency spectra of (a) $NaHSO_4$ and (b) Na_2SO_4 at 0.0, 0.005, 0.01, 0.02, and 0.03 bulk *X* in the OH stretching region at the vapor/H_2O interface acquired under *ssp*-polarization. (c) Resonant modes and overall fit to 0.03 bulk *X* $NaHSO_4$. (d) Resonant modes and overall fit to 0.03 bulk *X* Na_2SO_4. (e) Spectra of HCl (pH ∼ 0.5) and NaOH (pH ∼ 12) (inset). (f) Spectra of Na_2SO_4 (0.005, 0.01, 0.02, and 0.03 *X*) at a constant ionic strength (5 M).

solutions show solvation features at ∼3590 and 3625 cm^{-1}, respectively.[52]

The presence of large polarizable anions also affects the nonresonant response. VSF spectra of the salts in D_2O were acquired in the OH stretching region. Because there are no vibrational resonances from OD stretching in the OH stretching region, any change in intensity is attributed to a change in the nonresonant response. Compare the spectrum of Na_2SO_3 in D_2O at 0.03 *X* to the spectrum of the neat D_2O interface in the OH stretching region in Figure 4b. There is a nonnegligible increase in the nonresonant intensity. The nonresonant response from low salt concentrations (less than 0.01 *X*) could not be distinguished from the neat D_2O intensity. Increases in the nonresonant response for solutions ≥0.01 *X* interfere constructively with the tetrahedrally coordinated OH stretching region *exaggerating* these modes. Even with this increase in nonresonant intensity, the spectral fits confirm that most of the intensity changes in the spectra are in the resonant modes of the strongly bonded peaks (3200 and 3330 cm^{-1}) for both $NaHSO_3$ and Na_2SO_3.

$NaHSO_4$ and Na_2SO_4. Concentration series from 0.001 to 0.03 *X* of $NaHSO_4$ and Na_2SO_4 in *ssp*-polarization are presented in Figure 5a and 5b, respectively. A neat water spectrum (blue) is shown for comparison, and spectral fits for the highest salt concentrations are provided in Figure 5c,d. Like $NaHSO_3$ and Na_2SO_3, the most prominent change with increasing concentration of both compounds occurs in the strongly coordinated OH stretch region below 3400 cm^{-1}. The increase in spectral intensity is due to an increased contribution from the strongly coordinated and tetrahedrally bonded water molecules at 3330 and 3200 cm^{-1} with contributions from the 3150 cm^{-1} resonance at higher concentrations. Increases in these OH stretching modes are attributed to strong ion−dipole interactions (increasing the transition strength) and an enhanced oriented water network at the interface aligned with the increased interfacial electric field. This increase in intensity at longer wavelengths has been observed previously for sulfate-containing solutions,[60,61] and surface water bound as hydrates has been proposed for high concentrations of H_2SO_4.[62]

The largest difference between the sulfate and sulfite solutions in *ssp*-polarization spectra appears near 3460 cm^{-1}. Both sulfate-containing solutions show an enhancement in this spectral intensity with the largest effect observed for $NaHSO_4$ as determined from spectral fitting. At 0.02 and 0.03 *X* $NaHSO_4$, the intensity in the donor OH region increases (14 and 18%, respectively) and decreases slightly in the free OH mode (∼14%) indicating that the water molecules in the top interfacial layer, straddling the interface, are perturbed by the presence of these ions in solution. (From the fits to the data, all changes to the free OH mode are within the fitting error until the

(60) Shultz, M. J.; Schnitzer, C.; Simonelli, D.; Baldelli, S. *Int. Rev. Phys. Chem.* **2000**, *19*, 123−153.
(61) Gopalakrishnan, S.; Jungwirth, P.; Tobias, D. J.; Allen, H. C. *J. Phys. Chem. B* **2005**, *109*, 8861−8872.
(62) Shultz, M. J.; Baldelli, S.; Schnitzer, C.; Simonelli, D. *J. Phys. Chem. B* **2002**, *106*, 5313−5324.

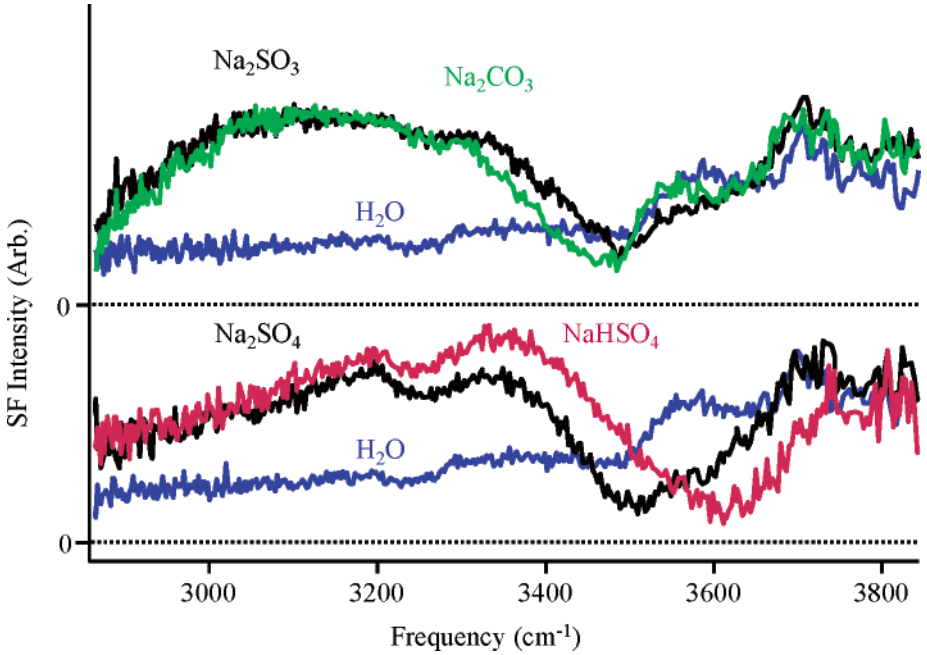

Figure 6. Sum-frequency spectra of Na_2SO_3, Na_2CO_3, Na_2SO_4, and $NaHSO_4$ at 0.03 *X* in the OH stretching region at the vapor/H_2O interface acquired under *sps*-polarization with a neat vapor/water spectrum in blue.

concentrations are ≥0.02 *X*.) The pH of the 0.03 *X* solutions is ~1 and 8 for $NaHSO_4$ and Na_2SO_4, respectively. In addition to the sodium ions in the interfacial region, the concentration of protons is substantial (0.1 M) for $NaHSO_4$. Very small contributions from solvating water molecules are included at higher concentrations to improve the fits.

To investigate what role the pH has in the differences between the $NaHSO_4$ and Na_2SO_4 spectra in Figure 5, spectra were acquired in pure water from pH 1 to pH 12 by additions of HCl or NaOH. Changes in the vapor/water spectra were observed near pH 1 and above pH 12. In Figure 5e, a spectrum of the HCl/water interface at pH ~1 in *ssp*-polarization is shown. At low pH, the HCl spectra show changes similar to that observed for $NaHSO_4$ (Figure 5a). The increase in spectral intensity covers a broad frequency range, and we attribute the enhancement of the lower-frequency features (3150, 3200, and 3330 cm^{-1}) to an enhanced electric field effect and strong electrostatic interactions between water molecules and protons in solution. Broad H_3O^+ ν_1 and ν_3 vibrations have been attributed to features in the 2900−3400 cm^{-1} region.[63−65] This enhancement in signal at lower frequencies has been observed in previous SF studies of acidic solutions and attributed primarily to an enhanced electric field effect causing an increase in signal at the lower frequencies.[47] For the highly acidic solution (Figure 5c), we attribute additional increases in the 3400−3500 cm^{-1} region to water molecules weakly solvating protons and water molecules at the surface with fewer hydrogen-bond interactions. Isotopic dilution studies of acid solutions that further characterize these protonated species in this spectral region will appear in a future publication. The similarity in changes in this region with the $NaHSO_4$ spectrum of Figure 5a suggests that similar protonated species are affecting the topmost surface layer of the $NaHSO_4$-containing solution. Evidence for hydrated protons in the interfacial region has been presented in recent SHG experiments[66] and MD simulations.[55]

At pH 12 (Figure 5e inset), the spectrum shows that the hydroxide ion concentration does not affect the water structure. No spectral changes were observed for the NaOH/water interface until the pH was greater than 12. At this point, the addition of NaOH leads to a more random orientation of water molecules evidenced by the lower intensity throughout the OH stretching region.

Because the salt solutions were acquired with varying ionic strength, a constant ionic strength series of Na_2SO_4 at the vapor/water interface was also acquired (Figure 5f). The ionic strength was held constant at ~5 M with sodium chloride. NaCl was chosen because the strength, orientation, and coordination of hydrogen bonds at the NaCl/water interface have been shown to be very similar to the hydrogen bonding at the neat vapor/water interface for 0.03 *X* solutions.[26] We were not able to determine the exact effect of increasing the ionic strength because the anion present in greatest concentration determined the interfacial water structure. For example, the Na_2SO_4/NaCl/water interface closely resembles the NaCl/water interface at low Na_2SO_4 concentrations and closely resembles the Na_2SO_4/water interface at high Na_2SO_4 concentrations. At this high ionic strength, charge separation should be on the order of a few angstroms, indicating that the increase in intensity in this region due to the sulfate ion is not solely an electric field effect. Interestingly, the results show that the type of anion present has a greater effect than the amount of surface charge. We assume for all the salts studied that the differences in the spectra are due to the different anions (with the exception of the influence of pH on the $NaHSO_4$ solutions). Variations in ionic strength do not have a significant effect on the interfacial water molecules.

(63) Bethell, D. E.; Sheppard, N. *J. Chem. Phys.* **1953**, *21*, 1421−1421.
(64) Stoyanov, E. S.; Hoffmann, S. P.; Kim, K.-C.; Tham, F. S.; Reed, C. A. *J. Am. Chem. Soc.* **2005**, *127*.
(65) Falk, M.; Giguere, P. A. *Can. J. Chem.* **1957**, *35*, 1195−1204.
(66) Petersen, P. B.; Saykally, R. J. *J. Phys. Chem. B* **2005**, *109*, 7676−7980.

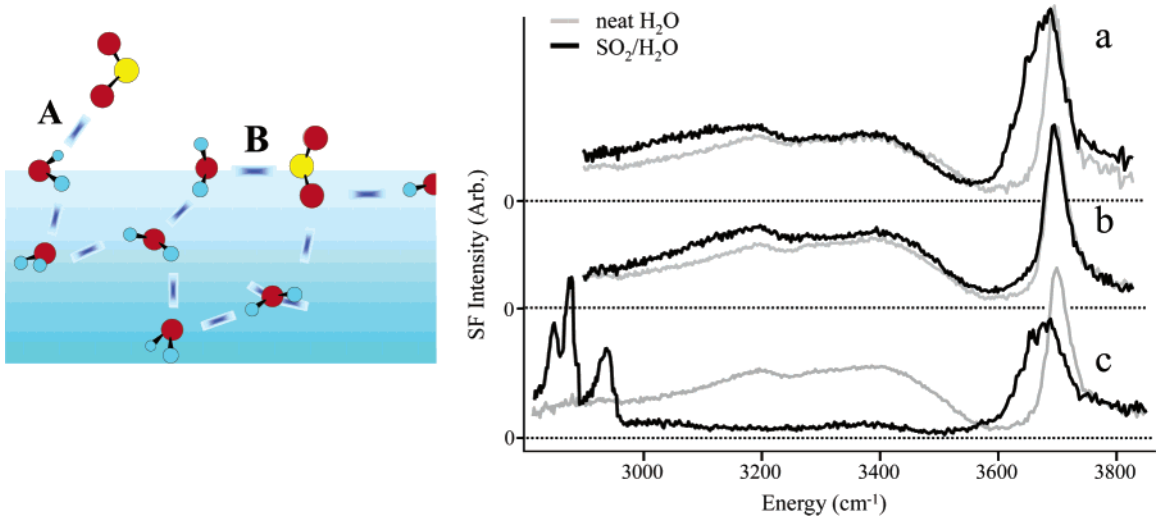

Figure 7. Adapted from *J. Am. Chem. Soc.* **2005**, *127*, 161806. Left: a cartoon of the SO_2/air/water interface. Possible SO_2:H_2O complexes are depicted: **A**, the oxygen of SO_2 bonding to the hydrogen atom of water, and **B**, the sulfur atom of SO_2 bonding to the oxygen atom of water. Right: sum-frequency spectra of SO_2 gas at the vapor/water interface in the OH stretch region in *ssp*-polarization. (a) SO_2 gas is flowing (black). Neat vapor/water spectrum (gray). (b) Immediately after SO_2 gas is turned off (black). Neat vapor/water spectrum (gray). (c) SO_2 gas with organic contaminates present (black). Neat vapor/water spectrum (gray).

The *sps*-polarization spectra for 0.03 bulk mole fraction Na_2SO_3, Na_2CO_3, $NaHSO_4$, and Na_2SO_4 are offset in Figure 6 with a neat vapor/water spectrum in blue for comparison. The *sps*-polarization spectra for the salts are fit with the same OH stretching modes as those discussed in the *ssp*-polarization spectra with the exception of an additional resonance at 3580 cm^{-1}. The *sps*-polarization spectra support the conclusions drawn from the *ssp*-polarization data for all spectra, and the similarities suggest that orientation is not the dominating effect. Large increases in intensity are found for all salts in the tetrahedrally coordinated hydrogen-bonded region (3000−3400 cm^{-1}), consistent with a charged interfacial region (that enhances both types of highly coordinated contributing modes) and with ion−dipole contributions such as those observed for Na_2SO_4. In the weaker bonding region of 3500−3700 cm^{-1} corresponding to the more labile (less weakly bound) water molecules, the largest effect in the *sps*-polarization data is observed for $NaHSO_4$ and Na_2SO_4, where the additional broadening of the 3460 cm^{-1} mode significantly interferes with the signal from the largely in-plane water molecules near 3580 cm^{-1}. We attribute these spectral variations in this region for the sulfate-containing solutions to small changes in orientation of these topmost weakly bound water molecules as they solvate ionic species in the surface region including protons for the $NaHSO_4$ and possibly the $NaHSO_3$ solution. The minimal change in the *sps*- and *ssp*-polarization spectra in this weakly bonded region for Na_2SO_3 indicates a smaller effect from these ions on the topmost layer. The Na_2CO_3 solution data will be discussed later.

Interestingly, these results are in direct contrast to the results from sodium halide salts where large anions showed significant increases in weak solvation features but not large increases from strong ion−dipole interactions and cooperative tetrahedrally coordinated stretching. Overall, the anions presented here are capable of hydrogen bonding and strong ion−dipole interactions that suggest these ions are strongly solvated in the interfacial region.

SO_2 at the Vapor/Water Interface. Figure 7 compares the VSF spectrum of the neat water surface during and after exposure to SO_2. In the presence of SO_2, an enhancement throughout most of the OH stretching region (3150−3500 cm^{-1}) is observed including the modes at 3200, 3330, and 3460 cm^{-1}. As seen above, these increases in intensity can be attributed to the presence of H^+ and HSO_3^-, which lead to spectral increases in the 3200, 3330, and 3460 cm^{-1} modes. Protons ellicit strong electrostatic interactions, and HSO_3^- has strong ion−dipole interactions with water and/or enhances the water network. SO_3^{2-} also increases the tetrahedrally coordinated OH stretching region, but the contribution is likely insignificant at the SO_2/water interface because of its low concentration ($\sim 10^{-5}$ M) at the measured pH of 1.

When SO_2 gas is present, the broadening of the free OH mode can be fit to an additional mode present at 3675 cm^{-1} that was not observed in any of the salt solutions, even at high salt concentrations. This new feature indicates an uncharged weak hydrogen-bonding interaction between SO_2 gas and water molecules in the top surface layer. This mode is assigned to an SO_2:H_2O surface complex (see the cartoon in Figure 7). There are similarities between the free OH mode and the surface complex OH mode. In the interfacial region, more than 20% of the H_2O molecules have free OH oscillators which collectively give rise to a distinct, sharp feature that is on average oriented out of the surface plane. The shape and phase of the mode from the complex are the same as those of the free OH; it is a relatively sharp feature that is on average pointed out of the plane of the interface. The lower peak frequency of the surface complex suggests a bonding interaction, and broadening suggests an increase in the number of bonding environments. Support for this mode as a surface complex is seen by considering the spectrum in Figure 7b, which presents the SO_2:H_2O spectrum without SO_2 gas flowing through the cell during the measurement. The SF spectrum in Figure 7b was acquired immediately after the gas was turned off. There is no longer a feature at 3675 cm^{-1}. This occurs as SO_2 gas leaves the surface, either through SO_2 outgassing or SO_2 reacting with water to form HSO_3^-. Even though the bulk pH is the same, without the atmosphere of SO_2, the feature is not observed. Uptake measurements suggest that the binding energy of the complex to the surface is small, ~12 kcal/mol.[8]

There are two possibilities for bonding in a 1:1 SO_2:H_2O surface complex, an oxygen in SO_2 bonding to the hydrogen atom of water (Figure 7A) or the sulfur atom of SO_2 bonding to the oxygen atom of water (Figure 7B). In the first case, water acts as a π-electron acceptor (hydrogen-bonding interaction). The out-of-plane orientation of the new OH resonance in the SF experiments suggests that this complex is bound through the oxygen of SO_2 and the hydrogen of H_2O. Because the SO_2 interacts with a water molecule straddling the interface, this type of interaction would be most probable, if the only consideration is the number of ways this interaction could be spatially accommodated. Evidence for both of these interactions, water acting as a lone-pair donor and a π-electron acceptor, has been seen in low-temperature matrix and FTIR film studies.[67,68] The N_2 matrix isolation studies show a 14 cm^{-1} shift from the ν_3 (antisymmetric stretch) at 3725 cm^{-1} of the water monomer to the same stretch in the SO_2:H_2O complex at 3711 cm^{-1}.[69] The second case is a lower-energy configuration based on gas-phase ab initio calculations[9] and microwave spectra results[70] where water acts as a lone pair donor toward the sulfur of SO_2, effectively making the hydrogen atom of the water molecule more acidic which red shifts the unbound OH mode (Figure 7B). This configuration is termed the sandwich structure (C_s symmetry) with ~44° between the planes of the two molecules.[11] In the sum-frequency spectra, the orientation of the surface water molecule that interacts with SO_2 has one hydrogen atom out of the interfacial plane; therefore, the sandwich structure would require the SO_2 to also straddle the interfacial plane inducing interactions with other water molecules. In the interfacial region, this interaction would be more probable between SO_2 and an acceptor water molecule (with both hydrogen atoms pointed toward the bulk) or if the water molecule has both hydrogen atoms near the plane of the interface as not to sterically hinder the S−O interaction. If SO_2 molecules straddle the interface similar to the free OH, additional interactions with water molecules are likely.

It is interesting to note that matrix studies have observed 1:1, 1:2, and 2:1 SO_2:H_2O complexes with a variety of proposed bonding environments.[67] It is not surprising, given the large first-order rate constant and solubility, that various bonding interactions are possible. The matrix studies suggest that a 1:1 interaction with either geometry is possible and that other stoichiometries of SO_2:H_2O complexes exist. Therefore, even though the orientation of the water mode is out of the plane of the interface, additional overlapping modes from larger complexes may contribute to the intensity.

There is a small (5 cm^{-1}) blue shift in the donor OH mode (within the uncertainty in fitting the data) that accompanies the out-of-plane complex mode. MD simulations of the air/water interface in our group suggest that the stretching modes from water molecules that straddle the interface are not strongly coupled because of their very different environments. Therefore, the change in the donor OH is not large in part because of the uncoupled nature of a straddling water molecule (presumably, it is still hydrogen bonded).

The SF experiments do not show any evidence for a surface complex from $NaHSO_3$ solutions that evolve SO_2, unlike the SHG experiments.[10] The bound SO_2 mode is present in the sum-frequency spectra only when water is in an atmosphere of SO_2 gas and the gas is continually flowing. When the surface is saturated with SO_2 gas and the flow of gas is ceased, the sample outgasses and the free OH mode grows in and resembles that of the neat vapor/water interface (Figure 7b). Dissolved SO_2, HSO_3^-, and SO_3^{2-} are still present and detectable by pH measurements and in the SF response. In contrast, solutions of aqueous sodium bisulfite (with dissolved SO_2) do not show this same high-frequency broad OH stretching feature because the amount of SO_2 evolving is not detectable with sum-frequency in this wavelength region. We agree that the species causing the SHG enhancement is probably the same that is producing the surface tension decrease, but it is not likely to be a surface SO_2:H_2O species.

Interestingly, we observe the SO_2:H_2O complex even in the presence of organic contaminants (Figure 7c). This is a significant result because recent models of aerosols include a significant organic component. In the presence of organic contaminants introduced by impurities in the gas samples, CH stretch modes of the contaminants appear in the 2900 cm^{-1} region. Most of the OH stretching modes disappear because of adsorption of contaminants on the top layer, but the complexed OH mode is still present and broad. SO_2 is still able to form a hydrate and adsorb at this interface. Similarly, the interfacial region of an aerosol composed of SO_2 and water would be covered with organic molecules. Where water molecules straddle the interface, this interaction between SO_2 and water can still occur.

In summary, the product anions of the SO_2 and water reaction enhance the OH stretching modes, especially the highly coordinated modes at 3330 and 3200 cm^{-1}. Protons also enhance the OH stretching modes of the tetrahedrally coordinated stretching throughout the symmetric OH modes typical of liquid water (including the 3460 cm^{-1} donor OH mode). SO_2 at the vapor/water interface shows evidence for a weak surface complex. This complex is attributed mainly to a 1:1 surface complex.

$NaHCO_3$, Na_2CO_3, and CO_2 at the Vapor/Water Interface. SO_2 and CO_2 have reaction products of different sizes and geometries, but the spectral interpretations of the $NaHCO_3$ and Na_2CO_3/water interfaces are very similar to those for the $NaHSO_3$ and Na_2SO_3/water interfaces. Spectra of the reaction product salts at the vapor/water interface in *ssp*-polarization are presented in Figure 8. The top spectra include the neat vapor/water interface, 0.01, and 0.02 *X* $NaHCO_3$, and the bottom spectra include the neat vapor/water interface, 0.001, 0.005, 0.01, 0.02, and 0.03 *X* Na_2CO_3. The pH is approximately 5 and 12 for $NaHCO_3$ and Na_2CO_3 at 0.02 and 0.03 *X*, respectively, and as seen previously, this change in pH does not affect the neat vapor/water spectrum.

$NaHCO_3$ is only soluble to approximately 0.02 *X* and has the smallest effect on the water structure of all the salts examined at the vapor/water interface. The OH stretching modes at 0.005 *X* $NaHCO_3$ are very similar to the OH stretching modes of the neat vapor/water interface. The increases in intensity with

(67) Schriver, A.; Schriver, L.; Perchard, J. P. *J. Mol. Spectrosc.* **1988**, *127*, 125−142.
(68) Schriver-Mazzuoli, L.; Chaabouni, H.; Schriver, A. *J. Mol. Struct.* **2003**, *644*, 151−164.
(69) Scherer, J. R. *Advances in Infrared and Raman Spectroscopy*; Heyden: London, 1978; Vol. 5.
(70) Matsumura, K.; Lovas, F. J.; Suenram, R. D. *J. Chem. Phys.* **1989**, *91*, 5887−5894.

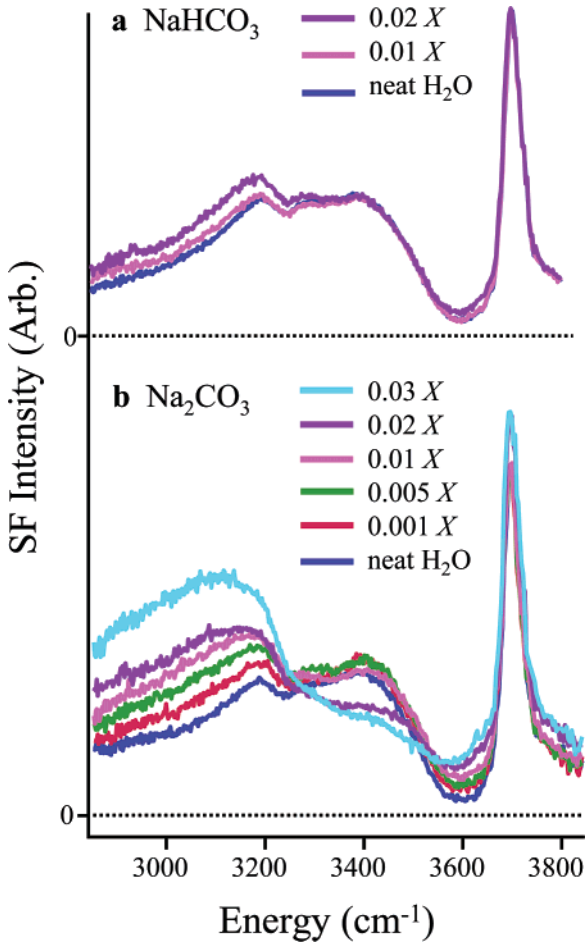

Figure 8. (a) Sum-frequency spectra of $NaHCO_3$ at 0.0, 0.1, and 0.2 *X* at the vapor/H_2O interface acquired under *ssp*-polarization. (b) Sum-frequency spectra of Na_2CO_3 (bottom) at 0.0, 0.005, 0.01, 0.02, and 0.03 bulk *X* in the OH stretching region at the vapor/H_2O interface acquired under *ssp*-polarization.

increasing concentration in the highly coordinated water modes are the same as those seen for $NaHSO_3$, and the interpretation is the same. This is due to strong ion−dipole interactions and an alignment of dipoles and/or an increase in the number of molecules aligned in the field.

Comparing similar concentrations, Na_2CO_3 has a greater effect than $NaHCO_3$ on the vapor/water interface because of the greater anion charge. There is a considerable increase in the coordinated OH stretching corresponding to the 3330 and 3200 cm^{-1} modes with contributions from the 3150 cm^{-1} mode at higher bulk concentrations. At 0.02 and 0.03 bulk mole fractions of Na_2CO_3, intensity in the donor OH mode (3460 cm^{-1}) decreases along with a small blue shift in the peak frequency and concomitant increases in the solvation OH stretch at 3645 cm^{-1}. This behavior is the same as that seen for Na_2SO_3 at the vapor/water interface, and the same interpretation is given. These ions are large, polarizable, and capable of hydrogen bonding to water molecules, directly affecting the water molecules in the interfacial region through ion−dipole interactions. Indirectly influenced by the ions, the interfacial water molecules align their dipoles with the field and/or a greater number of water molecules are affected in the presence of the field, increasing the cooperative OH stretching.

A spectrum of CO_2 at the vapor/water interface in *ssp*-polarization is shown in Figure 9. The CO_2/water interface has

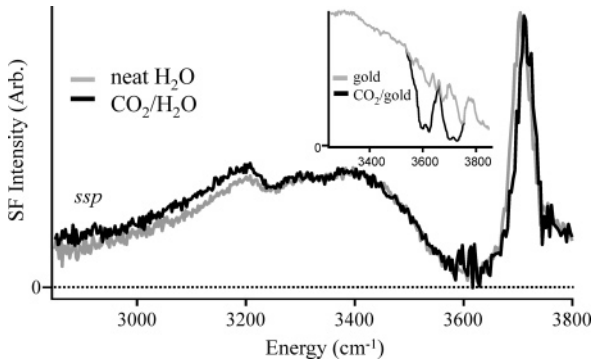

Figure 9. Sum-frequency spectra of CO_2 gas at the vapor/water interface in the OH stretch region in *ssp*-polarization. Inset: spectra of uncoated gold with and without CO_2 atmosphere present. There are two large CO_2 absorbances in the IR.

the same enhancements in the coordinated OH stretching region as those found in the SO_2/water spectrum. In the present case, the highly coordinated OH stretching increases because of the presence of the reaction products, H^+, HCO_3^-, and CO_3^{2-}. Although HCO_3^{2-} and CO_3^{2-} are present, the reaction of CO_2 with water occurs on a much slower time scale. CO_2 gas was delivered for approximately 45 min for significant changes in the coordinated OH stretching region to occur, which is consistent with the longer equilibration time. (SO_2, in contrast, enhances the coordinated stretching region as soon as the gas is delivered.) Recall that the overall effect on the water structure is smaller for $NaHCO_3$ than for $NaHSO_3$ at the same concentration; most likely because of their different geometries and pH. Spectra at the CO_2/water interface are different from those at the SO_2/water interface in the high-frequency region. There is a large decrease in the sum-frequency intensity of the nonresonant gold spectrum in Figure 9 (inset) at ∼ 3610 and 3710 cm^{-1} compared to the nonresonant gold spectrum without the atmosphere of CO_2. IR studies of H_2O + CO_2 (1:1) ice assign these spectral features to CO_2.[71] These absorbances in the IR are considerably broadened from the sharp CO_2 peaks in ice and cause the SF intensity to drop near zero. Although normalizing for this additional absorbance increases the fitting error in this region, a weak CO_2:H_2O complex was not observed. We assume the geometry and strength of the C═O bond is such that the probability of forming a complex is low. Overall, the spectrum closely resembles the spectrum at the neat vapor/water interface. Some dissolved CO_2 is present in the sample prior to the addition of CO_2 gas; however, boiling nanopure water prior to taking a sum-frequency spectrum of the neat interface in a closed N_2 purged cell did not significantly change the spectrum. The small amount of predissolved CO_2 does not appear to have an effect on the vapor/water interface.

Conclusions

The effects of SO_2 and CO_2 on the vapor/water interface were investigated by comparing OH stretching intensities in the neat interfacial water spectrum to OH stretching intensities when SO_2, CO_2, or various salts of the reaction and oxidation products of SO_2 and CO_2 were present. These salts include $NaHSO_3$, Na_2SO_3, $NaHSO_4$, Na_2SO_4, $NaHCO_3$, and Na_2CO_3.

Our studies clearly show the formation of a weakly bonded complex between SO_2 and the topmost surface water molecules

(71) Moore, M. H.; Khanna, R. K. *Spectrochim. Acta* **1991**, *47A*, 255−262.

when the water surface is exposed to SO_2 gas. The SO_2:H_2O complex is indicated by an OH resonance at 3675 cm^{-1}. This mode represents weak interactions between the water molecules straddling the interface and SO_2 molecules in the vapor phase, which are present in an atmosphere of SO_2. We attribute this feature to a 1:1 complex based on the phase and orientation of the molecules giving rise to the resonance; however, contributions from other hydrate complexes cannot be definitively ruled out. These studies show that SO_2 in particular has an immediate effect on the surface composition, which has implications for understanding the aerosol composition and structure. The complex between water and SO_2 remains when organic molecules are present in the interfacial region, which is directly relevant to atmospheric aerosols whose surfaces likely contain a significant organic component.

After the SO_2 gas has been removed, there is a measurable change in the surface water spectrum. We attribute these changes to the reaction products, HSO_3^-, SO_3^{2-}, and H^+. At high concentrations, all of the reaction products affect the topmost water layer where more labile water molecules reside. However, these species most significantly alter the orientation of the water molecules that are more strongly hydrogen bonded and reside slightly deeper in the interfacial region that can form more tightly bonded tetrahedrally coordinated complexes and couple more extensively to other water molecules. This occurs for all of the sulfur-containing ion solutions. We attribute the increased OH stretching intensity that occurs for all ions below 3400 cm^{-1} to strong ion−dipole interactions and ordering of water molecules in an electric field resulting in an increase in transition strength and interfacial depth. The protons present have an additional effect on the water molecules; they elicit strong electrostatic interactions and increase the intensity in the 3400−3500 cm^{-1} region, which we attribute to proton hydrate vibrations.

Over time, CO_2 also induces similar effects but no specific surface-bound species was observed. The adsorption of CO_2 gas to the neat vapor/water interface results in a significant but smaller change in intensity (than the adsorption of SO_2 gas) at the neat interface. The effect of CO_2 gas on the top monolayer (the free OH and donor OH modes of the molecules) was not detectable. The effect of protons in the interfacial region was not detectable in the pH range of these experiments. The ions formed in solution by the dissolution and reaction of the gases, primarily HCO_3^-, and small concentrations of CO_3^{2-} also affected the surface water structure, which included extending the interfacial region and imposing strong hydrogen bonding unlike the weaker effects of the halide ions.

Concentration studies of $NaHSO_3$, Na_2SO_3, Na_2SO_4, $NaHSO_4$, $NaHCO_3$, and Na_2CO_3 up to 0.03 *X* of sodium salt solutions illuminate new details about sulfur(carbon)-containing ions in the surface region. There are significant increases in intensity with increases in salt in the strongest hydrogen-bonding region of the spectrum, as has been seen previously. The greatest effects are from anions with greater charge. This is attributed to an increase in the cooperative stretching motion of tetrahedrally coordinated water molecules, which is consistent with the structure-making properties of associated ions in the Hofmeister series, strong ion−dipole interactions, and water molecules orienting in an electric field. The differences between the anions are most likely due to their different size and electronic distribution (geometry) in the interfacial region. In addition, some of the increase in intensity in the highly coordinated OH stretching region is from an increase in intensity in the nonresonant background and from protons when the pH is low (∼1).

There is also evidence for weak interactions between water molecules and ions at high ion concentrations, ≥ 0.01 *X*, in the topmost surface layer as observed through spectral changes and spectral fitting in the 3500−3700 cm^{-1} region for the *ssp*- and *sps*-polarization data. The orientation and bonding of water molecules in this weakly bonded region of the spectrum are impacted by the presence of sulfur-containing ions. High ionic strength studies show that this is not merely an electrostatic double-layer field effect. The electron distribution (geometry) of the anion affects the OH stretching differently. Spectral fitting indicates that water molecules solvating these anions are present in these topmost layers. For the $NaHSO_4$ solutions, there is evidence that solvated protons affect the topmost layer as recently theorized.[55]

Acknowledgment. The authors thank the National Science Foundation (CHE 0243856) for supporting this research and the Office of Naval Research for instrumentation.

JA057375A